Chapter 7
Distributed Event-Based Control for Interconnected Linear Systems

María Guinaldo, Dimos V. Dimarogonas, Daniel Lehmann and Karl H. Johansson

7.1 Introduction

One way to study the control properties of large-scale systems is to consider that the plant is composed of interconnected systems. The motivation for this assumption is twofold. On the one hand, physical plants are made up of parts, which can be identified as different subsystems, and this structural feature can facilitate the control design. On the other hand, even if the system does not present these physical boundaries, it might be useful to decompose it into mathematical subsystems which have no obvious physical identity. These terms of physical and mathematical decomposition were first introduced by Siljak [236], and since then they have been used in the design of centralized and distributed controllers.

Practical examples of these large-scale systems are power or traffic networks, in which a centralized solution would require a very powerful network and an accurate model of all the interconnections, and moreover, it would be not robust against node failures, for example. The design of decentralized controllers for this kind of systems is a suboptimal solution since it does not take into account the interconnection between the subsystems. Hence, there is a natural interest in applying distributed

M. Guinaldo (✉)
Dpto. de Informática y Automática, Escuela Técnica Superior de Informática, UNED, Madrid, Spain
e-mail: mguinaldo@dia.uned.es

D.V. Dimarogonas, D. Lehmann and K.H. Johansson
School of Electrical Engineering, Royal Institute of Technology (KTH), Stockholm, Sweden
e-mail: dimos@kth.se

D. Lehmann
e-mail: dlehmann@kth.se

K.H. Johansson
e-mail: kallej@kth.se

M. Guinaldo Losada et al. (eds.), *Asynchronous Control for Networked Systems*,
DOI 10.1007/978-3-319-21299-9_7

control to these scenarios, and, if the communication between the local controllers is event triggered, get better usage of the network.

There are some recent contributions on distributed event-triggered control [51, 54, 88, 166, 232, 259]. The basic idea in all these contributions is that each subsystem decides when to transmit the measurements based only on local information. In the most common implementations, an event is triggered when the error of the system exceeds a tolerable bound.

This chapter discusses different control strategies of distributed event-based controls for linear interconnected systems. Part of these results are based on the contributions [88, 89, 91]. Section 7.2 provides the mathematical tools used through the chapter as well as the problem statement. Different distributed trigger functions are examined in Sect. 7.3: deadband control, Lyapunov approaches, and exponential bounds, which is the proposal of the authors to the studied problem. Other existing strategies such as, for example, small-gain approaches [51] do not prevent from Zeno behavior, and a constant threshold-like condition must be included to overcome this issue, yielding similar results to the deadband control from the analytical point of view.

The analytical results are provided in Sect. 7.4. Two aspects are analyzed: Convergence to the equilibria and inter-event times, and the results are illustrated with an example in Sect. 7.4.3. The extension to discrete-time systems is given in Sect. 7.5.

Model-based approaches has been shown to help to reduce communication in centralized schemes (see Chaps. 4 and 6). Thus, one of the first improvements presented in Sect. 7.6 consists of a distributed model-based approach combined with event-triggered communications. However, reducing the number of transmissions in the network is not the only aspect that matters in distributed systems. For instance, the frequency of the control update allows a more efficient usage of the limited resources of embedded microprocessors. Whereas in a single control loop the reduction of communication usually implies the reduction of actuator updates, this does not necessary hold in distributed systems, especially if the number of neighbors is large. Thus, the second improvement presented in Sect. 7.6 accounts for both phenomena in the design.

7.2 Background and Problem Statement

7.2.1 Matrix and Perturbations Analysis

Let $A \in \mathbb{C}^{n\times n}$ be a complex matrix, and let us define

$$\kappa(A) = \|A\|\|A^{-1}\| \quad (0 \notin \lambda(A)), \tag{7.1}$$

$$\alpha_{max}(A) = \max\{\mathbb{R}e(\lambda) : \lambda \in \lambda(A)\}, \tag{7.2}$$

The matrix exponential of A is defined as $e^{At} = \sum_{k=0}^{\infty} \frac{(At)^k}{k!}$. Through this chapter, the stability of the system is proved using some hints that are summarized in this section to bound $\|e^{At}\|$.

7.2.1.1 Bounding the Matrix Exponential

In [245] various norms are discussed to bound the exponential. Three are of particular interest:

- **Log norms** If $\mu_{max}(A)$ is defined as $\mu_{max}(A) = \max\{\mu : \mu \in \lambda((A + A^*)/2)\}$, then
$$\|e^{At}\| \leq e^{\mu_{max}(A)t}.$$
An interesting corollary can be inferred from the property above. Let Y be an invertible matrix such that $A = YBY^{-1}$. It follows that
$$\|e^{At}\| = \|Ye^{Bt}Y^{-1}\| \leq \kappa(Y)e^{\mu_{max}(B)t}, \tag{7.3}$$
where $\kappa(Y)$ is defined according to (7.1).
Thus, assume that A is *diagonalizable*, i.e., there exists a matrix D, where $D = \text{diag}(\lambda_i(A))$, and a matrix V of eigenvectors, such that $A = VDV^{-1}$. From (7.3), it holds that
$$\|e^{At}\| \leq \kappa(V)e^{\mu_{max}(D)t} = \kappa(V)e^{\alpha_{max}(D)t} = \kappa(V)e^{\alpha_{max}(A)t}, \tag{7.4}$$
where $\alpha_{max}(A)$ is defined according to (7.2).
- **Jordan canonical form** Recall the Jordan decomposition theorem which states that if $A \in \mathbb{C}^{n\times n}$, then there exists an invertible matrix $X \in \mathbb{C}^{n\times n}$ such that
$$X^{-1}AX = J_{m_1}(\lambda_1) \times \cdots \times J_{m_1}(\lambda_p) \equiv J,$$
where
$$J_k \equiv J_{m_k}(\lambda_k) = \begin{pmatrix} \lambda_k & 1 & & 0 \\ 0 & \lambda_k & \ddots & \\ \vdots & & \ddots & 1 \\ 0 & 0 & \dots & \lambda_k \end{pmatrix} \in \mathbb{C}^{m_k\times m_k}, \quad k = 1, \dots, p.$$
By taking norms and defining $m = \max\{m_1, \dots, m_p\}$, it can be proved that [245]
$$\|e^{At}\| \leq m \cdot \kappa(X)e^{\alpha_{max}(A)t} \max_{0\leq r\leq m-1} \frac{t^r}{r!}. \tag{7.5}$$

Note that X may not be unique but it is assumed that it is chosen such that $\kappa(X)$ is minimized.

- **Schur decomposition bound** The Schur decomposition states that there exists a unitary $Q \in \mathbb{C}^{n\times n}$ such that

$$Q^* A Q = D + N, \tag{7.6}$$

where D is the diagonal matrix $D = \text{diag}(\lambda_i)$ and N is strictly upper triangular. The following upper bound can be obtained [245]

$$\|e^{At}\| \leq e^{\alpha_{max}(A)t} \sum_{k=0}^{n-1} \frac{\|Nt\|^2}{k!}. \tag{7.7}$$

7.2.1.2 Perturbation Bounds

The second aspect that is brought up in this section is the existing perturbation analysis on the eigenvalues and the matrix exponential, i.e., how the eigenvalues and the bound on the matrix exponential change when A is perturbed by E.

The following lemma merges classical results from [17, 44] to study the perturbation of the eigenvalues of a matrix A in two situations: when A is diagonalizable and when it is not.

Lemma 7.1 *If A is diagonalizable ($V^{-1}AV = D$), the eigenvalues $\tilde{\lambda}_i$ of $A + E$ satisfy*

$$\min_{\lambda_j \in \lambda(A)} |\tilde{\lambda}_i - \lambda_j| \leq \kappa(V)\|E\|. \tag{7.8}$$

Otherwise, Let consider the Schur decomposition (7.6). Then for $\tilde{\lambda}_i \in \lambda(A + E)$

$$\min_{\lambda_j \in \lambda(A)} |\tilde{\lambda}_i - \lambda_j| \leq max\{\theta_1, \theta_1^{1/n}\}, \tag{7.9}$$

where $\theta_1 = \|E\| \sum_{k=0}^{n-1} \|N\|^k$.

Finally, a result from semigroup theory (see [126]) states that if $\|e^{At}\| \leq ce^{\beta t}$ for some constants c and β, then

$$\|e^{(A+E)t}\| \leq ce^{(\beta + c\|E\|)t}. \tag{7.10}$$

7.2.1.3 Perturbation Analysis and Matrix Powers

In discrete-time systems, the matrix exponential is replaced by the matrix power. Thus, a bound on $(A+E)^p$ is required. We introduce the concept of *Fréchet derivative* for this purpose.

Definition 7.1 [108] Let $A, E \in \mathbb{C}^{n\times n}$. The Fréchet derivative of a matrix function f at A in the direction of E is a linear operator L_f that maps E to $L_f(A, E)$ such that

$$f(A + E) - F(A) - L_f(A, E) = \mathscr{O}(\|E\|^2),$$

for all $E \in \mathbb{C}^{n\times n}$. The Fréchet derivative may not exist, but if it does it is unique.

The following lemma characterize the Fréchet derivative of the function X^p.

Lemma 7.2 *[3] Let $A, E \in \mathbb{C}^{n\times n}$. If $L_{X^p}(A, E)$ denotes the Fréchet derivative of X^p at A in the direction of E, then*

$$L_{X^p}(A, E) = \sum_{j=0}^{p-1} A^{p-1-j} E A^j.$$

This means that the p power of $A + E$ is

$$(A + E)^p = A^p + \sum_{j=0}^{p-1} A^{p-1-j} E A^j + \mathscr{O}(\|E\|^2).$$

Then, it is a logical consequence the following

$$\|(A + E)^p\| \leq \|A^p\| + \|\sum_{j=0}^{p-1} A^{p-1-j} E A^j\| + \mathscr{O}(\|E\|^2). \tag{7.11}$$

7.2.2 Problem Statement

Consider a large-scale system that have been decomposed into N_a linear time-invariant subsystems. The dynamics of each subsystem is given by

$$\dot{x}_i(t) = A_i x_i(t) + B_i u_i(t) + \sum_{j\in\mathscr{N}_i} H_{ij} x_j(t), \quad \forall i = 1, \ldots, N_a \tag{7.12}$$

where the set of "neighbors" of the subsystem i $\mathscr{N}_i$ is the set of subsystems that directly drive agent i's dynamics, and H_{ij} is the interaction term between agent i and agent j, and $H_{ij} \neq H_{ji}$ might hold. The state x_i of the ith agent has dimension n_i, u_i is the m_i-dimensional local control signal of agent i, and A_i, B_i, and H_{ij} are matrices of appropriate dimensions.

In each node or subsystem, we can distinguish the dynamical part strictly speaking and a microprocessor in charge of monitoring the plant state and computing the control signal and the communication tasks (see Fig. 7.1).

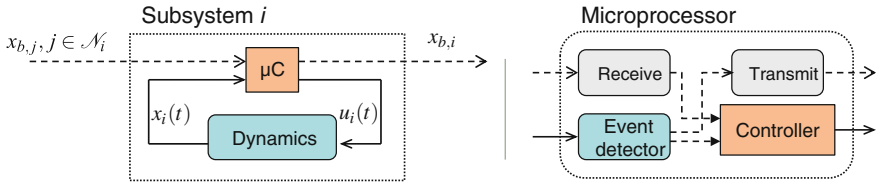

Fig. 7.1 Scheme of a node, consisting of a digital microcontroller (μC) and dynamics (*left*), and block diagram of the tasks carried out by the microprocessor

Due to the limited bandwidth, the communication between subsystems is at discrete instants of time. The dynamical coupling between subsystems makes it interesting to have access to the state of neighboring agents to include this information into the control law. Specifically, the agent i communicate with the set of agents in its neighborhood $\mathcal{N}_i$. The transmission occurs when an event is triggered. We denote by $\{t_k^i\}_{k=0}^{\infty}$ the times at which an event is detected in the agent i, where $t_k^i < t_{k+1}^i$ for all k.

The broadcast state is denoted by $x_{b,i}$. The broadcast states are used in the control law. Hence, the control signal is updated in a node, at least, when a new measurement is transmitted and/or received. In particular, the control law for each subsystem is

$$u_i(t) = K_i x_{b,i}(t) + \sum_{j \in \mathcal{N}_i} L_{ij} x_{b,j}(t), \quad \forall i = 1, \ldots, N_a \tag{7.13}$$

where K_i is the feedback gain for the nominal subsystem i. We assume that $A_i + B_i K_i$ is Hurwitz. L_{ij} is a set of decoupling gains.

Let us define the error $\varepsilon_i(t)$ between the state and the latest broadcast state as

$$\varepsilon_i(t) = x_{b,i}(t) - x_i(t) = x_i(t_k^i) - x_i(t), \quad t \in [t_k^i, t_{k+1}^i). \tag{7.14}$$

Rewriting (7.12) in terms of $\varepsilon_i(t)$ and the control law (7.13), we obtain

$$\dot{x}_i(t) = A_{K,i} x_i(t) + B_i K_i \varepsilon_i(t) + \sum_{j \in \mathcal{N}_i} \left(\Delta_{ij} x_j(t) + B_i L_{ij} \varepsilon_j(t) \right), \tag{7.15}$$

where $A_{K,i} = A_i + B_i K_i$, and $\Delta_{ij} = B_i L_{ij} + H_{ij}$ are the coupling terms. In general, $\Delta_{ij} \neq 0$ since the interconnections between the subsystems may be not well known, there might be model uncertainties or the matrix B_i does not have full rank.

We also define

$$A_K = \text{diag}(A_{K,1}, A_{K,2}, \ldots, A_{K,N_a}) \tag{7.16}$$

$$B = \text{diag}(B_1, B_2, \ldots, B_{N_a}) \tag{7.17}$$

$$K = \begin{pmatrix} K_1 & L_{12} & \cdots & L_{1N_a} \\ L_{21} & K_2 & \cdots & L_{2N_a} \\ \vdots & \vdots & \ddots & \vdots \\ L_{N1} & L_{N2} & \cdots & K_{N_a} \end{pmatrix} \tag{7.18}$$

$$\Delta = \begin{pmatrix} 0 & \Delta_{12} & \cdots & \Delta_{1N_a} \\ \Delta_{21} & 0 & \cdots & \Delta_{2N_a} \\ \vdots & \vdots & \ddots & \vdots \\ \Delta_{N_a1} & \Delta_{N_a2} & \cdots & 0 \end{pmatrix} \tag{7.19}$$

and the stack vectors

$$x = (x_1^T, x_2^T, \ldots, x_{N_a}^T)^T \tag{7.20}$$

$$\varepsilon = (\varepsilon_1^T, \varepsilon_2^T, \ldots, \varepsilon_{N_a}^T)^T \tag{7.21}$$

as the state and error vectors of the overall system. Note that $H_{ij}, L_{ij}, \Delta_{ij} := 0$ if $j \notin \mathcal{N}_i$. Let also be $n = \sum_{i=1}^{N} n_i$ the state and error dimension.

The dynamics of the overall system is given by

$$\dot{x}(t) = (A_K + \Delta)x(t) + BK\varepsilon(t). \tag{7.22}$$

As the broadcast states $x_{b,i}$ remain constant between consecutive events, the error dynamics in each interval is given by

$$\dot{\varepsilon}(t) = -(A_K + \Delta)x(t) - BK\varepsilon(t). \tag{7.23}$$

The above definition allows to study the stability of the overall system. These equations are valid as long as the following three time instances are simultaneous: the detection of the event, the transmission of the state $x_{b,i}$ from one node, and the reception in all neighboring nodes. When delays and packet dropouts can occur in the transmission, (7.22) and (7.23) do not generally hold. The extension to non-reliable communications is given in Chap. 10.

7.3 Event-Based Control Strategy

The design of distributed trigger functions $F_{e,i}$ to detect the occurrence of an event must satisfy the following properties:

- Guarantee the stability of the subsystem, and hence, of the overall system.
- Depend on local information of agent i only, or at most, of the neighbors, and take values in $\mathbb{R}$.

- Determine the sequence of local broadcasting times t_k^i recursively by the event-trigger function as $t_{k+1}^i = \inf\{t : t > t_k^i, F_{e,i}(t) > 0\}$.
- Ensure a lower bound for the inter-event times $T_{k,i} = t_{k+1}^i - t_k^i$.

In Chap. 1, the existing strategies for event-based control have been presented. Some of these approaches can be extended easily to distributed implementations. For instance, trigger functions for deadband control are

$$F_{e,i}(t) = \|\varepsilon_i(t)\| - \delta_i, \quad \delta_i > 0. \tag{7.24}$$

The design can be simplified by setting $\delta_i = \delta, \forall i = 1, \dots N_a$. Large values of δ allow reducing the number of events but degrades the performance. On the contrary, small values of δ give better performance but the average inter-event time decreases considerably. Moreover, this approach fails to ensure the asymptotic stability of the system, as in the case of centralized schemes.

Lyapunov-based sampling approaches to distributed event-triggering have also been studied. In this case, an event is enforced whenever

$$F_{e,i}(t) = \|\varepsilon_i(t)\| - \sigma_i \|x_i(t)\|, \quad 0 < \sigma_i < 1 \tag{7.25}$$

crosses from negative to positive. The set of parameters σ_i is determined by imposing that the Lyapunov function $V = \sum_{i=1}^{N_a} V_i(x_i)$ is locally positive definite and the time derivative of the Lyapunov-candidate-function is locally negative definite. For linear systems, the problem can be solved by solving a local LMI in each subsystem. See [259] for details. The asymptotic convergence to the equilibrium is guaranteed but a positive lower bound for the inter-event time may not be guaranteed when approaching the desired equilibria [79, 259].

In this chapter, the properties of trigger functions of the form

$$F_{e,i}(t) = \|\varepsilon_i(t)\| - \delta_{0,i} - \delta_{1,i} e^{-\beta_i t}, \quad \beta_i > 0 \tag{7.26}$$

are studied, where $\delta_{0,i}$ and $\delta_{1,i}$ cannot be zero simultaneously. To simplify the selection of parameters, we will consider that $\delta_{0,i} = \delta_0, \delta_{1,i} = \delta_1, \beta_i = \beta$, $\forall i = 1, \dots, N_a$.

Example 7.1 A trigger function (7.24) is depicted on Fig. 7.2a. The error is bounded by the constant threshold δ_0. Note that the error is reset after the occurrence of an event and that the inter-event time is always positive, since the error cannot reach the threshold again at the same time instance.
Trigger functions of the form (7.26) are represented on Fig. 7.2b. Note that the threshold decreases with time and the error is bounded by $\delta_0 + \delta_1$ at $t = 0$ and by δ_0 when $t \to \infty$. If $\delta_0 = 0$, this bound goes to zero when time increases and asymptotic stability can be achieved. Finally, Fig. 7.2c shows the error bound when events are enforced with (7.25).

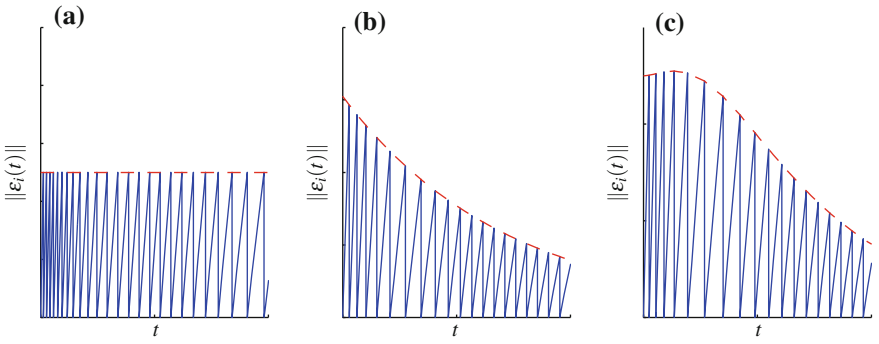

Fig. 7.2 Error function (*solid blue line*) and error bound (*dashed red line*) for trigger functions **a** (7.24), **b** (7.25), and **c** (7.26)

7.4 Performance Analysis

In this section, the stability properties of the system (7.12) are analyzed by using some of the results presented in Sect. 7.2.1. First, we briefly discuss the concepts of perfect and non-perfect decoupling that have some impact over the analytical treatment of the problem. After that the results are compared with other triggering mechanisms, and finally, this is also illustrated with a simulation example.

7.4.1 Perfect and Non-perfect Decoupling

If the decoupling gains L_{ij} can be chosen such that the *matching condition* holds, i.e., $\Delta_{ij} + B_i L_{ij} = 0$, (7.15) is transformed into

$$\dot{x}_i(t) = A_{K,i} x_i(t) + B_i K_i \varepsilon_i(t) + \sum_{j \in \mathcal{N}_i} B_i L_{ij} \varepsilon_j(t). \tag{7.27}$$

Hence, this essentially assures the perfect decoupling of the subsystems and allows to analyze their performance independently, since it holds that

$$x_i(t) = e^{A_{K,i}t} x_i(0) + \int_0^t e^{A_{K,i}(t-s)} \left(B_i K_i \varepsilon_i(s) + \sum_{j \in \mathcal{N}_i} B_i L_{ij} \varepsilon_j(s) \right) ds.$$

Then, if the error functions $\varepsilon_i(s)$, $\varepsilon_j(s)$ are bounded according to the trigger function (7.26), which are independent of the state, the convergence to the equilibrium only depends on local properties, that is, on the eigenvalues of $A_{K,i}$. Because the feedback gains K_i are designed so that $A_{K,i}$ is Hurwitz, the stability of each subsystem, and as a consequence, of the overall system, is guaranteed.

However, the perfect decoupling is a quite restrictive condition, and in many situations cannot be achieved because the interconnections between the subsystems may be not well known, there might be model uncertainties or the matrix B_i does not have full rank. Therefore, in the following, we assume that, in general, the interconnection terms $\Delta_{ij} \neq 0$.

In (7.22) Δ can be seen as a perturbation to A_K which influences the stability of the overall system. We obviously need to impose some constraints to Δ. Before doing this, the next assumption will facilitate the calculations in the following, but the extension to defective matrices is achievable as discussed later in the section.

Assumption 7.1 We assume that $A_{K,i}$, $i = 1, \ldots, N$ is diagonalizable so that there exists a matrix $D_i = \text{diag}(\lambda_k(A_{K,i}))$ and an invertible matrix of eigenvectors V_i such that $A_{K,i} = V_i D_i V_i^{-1}$.
The next lemma provides a bound for $\|\Delta\|$ that ensures that $A_K + \Delta$ is Hurwitz.

Lemma 7.3 *If $\kappa(V)\|\Delta\| < |\alpha_{max}(A_K)|$ holds, the eigenvalues $\tilde{\lambda}_i$ of $A_K + \Delta$ have negative real part.*

Proof According to the Bauer–Fike theorem (see (7.8) on p. 154), it follows that

$$\min_{\lambda_j \in \lambda(A_K)} |\tilde{\lambda}_i - \lambda_j| \leq \kappa(V)\|\Delta\|.$$

Assume that $\tilde{\lambda}_i = \tilde{\alpha}_i + i\tilde{\beta}_i$ and $\lambda_j = \alpha_j + i\beta_j$. Then, it holds that

$$|\tilde{\lambda}_i - \lambda_j| = \sqrt{(\tilde{\alpha}_i - \alpha_j)^2 + (\tilde{\beta}_i - \beta_j)^2} > |\tilde{\alpha}_i - \alpha_j|.$$

Because A_K is Hurwitz, $\alpha_j < 0, \forall j$, and according to the definition of $\alpha_{max}(A_K)$ (7.2), then it yields $|\alpha_{max}(A_K)| \leq |\alpha_j|, \forall j$. Moreover, if $\kappa(V)\|\Delta\| < |\alpha_{max}(A_K)|$, $\kappa(V)\|\Delta\|$ is also upper bounded by $|\alpha_j|, \forall j$. Thus, $\tilde{\alpha}_i$ is negative, because if it was positive

$$|\tilde{\alpha}_i - \alpha_j| = \tilde{\alpha}_i + |\alpha_j| > |\alpha_j| \geq |\alpha_{max}(A_K)| > \kappa(V)\|\Delta\|,$$

that would contradict the theorem of Bauer–Fike. Hence, $\tilde{\alpha}_i$ is negative, and this concludes the proof.

The previous result imposes a constraint over $\|\Delta\|$ to guarantee stability, and hence, an additional assumption is required.

Assumption 7.2 The coupling terms Δ_{ij} are such that $\kappa(V)\|\Delta\| < |\alpha_{max}(A_K)|$ holds.

The following theorem states that if Assumptions 7.1 and 7.2 hold, the system (7.22) with trigger functions defined as in (7.26) converges to a specified region around the equilibrium point which, without loss of generality, is assumed to be $(0, \ldots, 0)^T$. Moreover, if $\delta_0 = 0$ the convergence is asymptotical to the origin. The functions (7.26) bound the errors $\|\varepsilon_i(t)\| \leq \delta_0 + \delta_1 e^{-\beta t}$, since an event is triggered as soon as

the norm of $\varepsilon_i(t)$ crosses the threshold $\delta_0 + \delta_1 e^{-\beta t}$. The proof can be found in Appendix A.

Theorem 7.1 *Consider the closed-loop system (7.22) and trigger functions of the form (7.26), with $0 < \beta < |\alpha_{max}(A_K)| - \kappa(V)\|\Delta\|$. Then, if Assumptions 7.1 and 7.2 hold, for all initial conditions $x(0) \in \mathbb{R}^n$, and $t > 0$, the state of the overall system is upper bounded as follows:*

$$\begin{aligned}\|x(t)\| \leq & \kappa(V)\Bigg(\frac{\|BK\|\sqrt{N_a}\delta_0}{|\alpha_{max}(A_K)|-\kappa(V)\|\Delta\|} + e^{-(|\alpha_{max}(A_K)|-\kappa(V)\|\Delta\|)t}\Bigg(\|x(0)\|- \\ & \|BK\|\sqrt{N_a}\left(\frac{\delta_0}{|\alpha_{max}(A_K)|-\kappa(V)\|\Delta\|} + \frac{\delta_1}{|\alpha_{max}(A_K)|-\kappa(V)\|\Delta\|-\beta}\right)\Bigg) \\ & + e^{-\beta t}\frac{\|BK\|\sqrt{N_a}\delta_1}{|\alpha_{max}(A_K)|-\kappa(V)\|\Delta\|-\beta}\Bigg).\end{aligned} \tag{7.28}$$

Furthermore, the inter-event times are lower bounded by

$$T_{min} = \frac{\delta_0}{k_1 + k_2 + k_3}, \tag{7.29}$$

where

$$k_1 = \kappa(V)\|A_K + \Delta\|\|x(0)\| \tag{7.30}$$

$$k_2 = \|BK\|\sqrt{N_a}\delta_1\left(\frac{\kappa(V)\|A_K + \Delta\|}{|\alpha_{max}(A_K)| - \kappa(V)\|\Delta\| - \beta} + 1\right) \tag{7.31}$$

$$k_3 = \|BK\|\sqrt{N_a}\delta_0\left(\frac{\kappa(V)\|A_K + \Delta\|}{|\alpha_{max}(A_K)| - \kappa(V)\|\Delta\|} + 1\right). \tag{7.32}$$

Remark 7.1 The results of Theorem 7.1 can be particularized to the perfect decoupling case. The state is upper bounded by

$$\begin{aligned}\|x(t)\| \leq & \kappa(V)\Bigg(\frac{\|BK\|\sqrt{N_a}\delta_0}{|\alpha_{max}(A_K)|} + e^{-|\alpha_{max}(A_K)|t}\Bigg(\|x(0)\|- \\ & \|BK\|\sqrt{N_a}\left(\frac{\delta_0}{|\alpha_{max}(A_K)|} + \frac{\delta_1}{|\alpha_{max}(A_K)|-\beta}\right)\Bigg) \\ & + e^{-\beta t}\frac{\|BK\|\sqrt{N_a}\delta_1}{|\alpha_{max}(A_K)|-\beta}\Bigg),\end{aligned}$$

and the minimum inter-event times lower bounded by

$$\frac{\delta_0}{\kappa(V)\|A_K\|\|x(0)\| + \|BK\|\sqrt{N_a}\left(\delta_1\left(\frac{\kappa(V)\|A_K\|}{|\alpha_{max}(A_K)|-\beta} + 1\right) + \delta_0\left(\frac{\kappa(V)\|A_K\|}{|\alpha_{max}(A_K)|} + 1\right)\right)}.$$

Thus, when the matching condition holds, the rate of convergence to the equilibrium is faster and the minimum inter-event times larger.

Remark 7.2 If Assumption 7.1 does not hold, the results can be extended noting that $\|e^{A_K t}\|$ can be bounded by either using the Jordan Canonical form, and hence (7.5) holds, or the Schur decomposition bound (7.7). In both cases the bound is governed by the exponential of $\alpha_{max}(A_K)$, which is negative. Thus, the stability of the system is guaranteed though the speed of convergence to the equilibria decreases. Moreover, if A_K is defective, then the restraint over Δ that guarantees that the eigenvalues of $A_K + \Delta$ have negative real part can be obtained from (7.9), enforcing $\max\{\theta_1, \theta_1^{1/n}\} < |\alpha_{max}(A_K)|$.

7.4.2 Comparison with Other Triggering Mechanisms

The results derived previously can be compared to the most frequently used event-triggered control strategies. We also particularized the results for the case $\delta_0 = 0$, which is interesting since yields asymptotic stability.

7.4.2.1 Deadband Control

In deadband control, an event is triggered whenever the state crosses some levels defined by a constant. From the analytical point of view, this is equivalent to have trigger functions (7.26) with $\delta_1 = 0$ and the error bounded by $\|\varepsilon_i(t)\| \leq \delta_0$. Thus, from Theorem 7.1 bound for the state is

$$\|x(t)\| \leq \kappa(V)\left(\frac{\|BK\|\sqrt{N_a}\delta_0}{|\alpha_{max}(A_K)|-\kappa(V)\|\Delta\|} + e^{-(|\alpha_{max}(A_K)|-\kappa(V)\|\Delta\|)t}\left(\|x(0)\| - \|BK\|\sqrt{N_a}\frac{\delta_0}{|\alpha_{max}(A_K)|-\kappa(V)\|\Delta\|}\right)\right),$$

and a lower bound for the inter-event time is

$$T_{min} = \frac{\delta_0}{k_1 + k_3}.$$

7.4.2.2 Pure Exponential Trigger Functions

A particular case of trigger functions (7.26) is when $\delta_0 = 0$. For this situation, the state is upper bounded as

$$\|x(t)\| \leq \kappa(V)\left(e^{-(|\alpha_{max}(A_K)|-\kappa(V)\|\Delta\|)t}\left(\|x(0)\| - \frac{\|BK\|\sqrt{N_a}\delta_1}{|\alpha_{max}(A_K)|-\kappa(V)\|\Delta\|-\beta}\right) + e^{-\beta t}\frac{\|BK\|\sqrt{N_a}\delta_1}{|\alpha_{max}(A_K)|-\kappa(V)\|\Delta\|-\beta}\right).$$

Note that $\|x(t)\| \to 0$ when $t \to \infty$.

The expression that provides the solution of the minimum inter-event times is not derived directly from (7.29), and is given by

$$\left(\frac{k_1}{\delta_1}e^{(\beta-|\alpha_{max}(A_K)|)t^*}+\frac{k_2}{\delta_1}\right)T=e^{-\beta T}. \tag{7.33}$$

The right-hand side of (7.33) is always positive. Moreover, for $\beta < |\alpha_{max}(A_K)|$ the left-hand side is strictly positive as well, and the term in brackets is upper bounded by $\frac{k_2+k_1}{\delta_1}$ and lower bounded by k_2/δ_1, and this yields to a positive value of T for all $t^* \geq 0$. The proof can be found in Appendix A.

7.4.2.3 Lyapunov-Based Sampling

In [257], the problem presented in this chapter is addressed with trigger functions (7.25). The asymptotic stability of the system is guaranteed if there exists positive definite matrices P_i, Q_i such that

$$A_{K,i}^T P_i + P_i A_{K,i} \leq -Q_i$$
$$W_i = \sum_{j\in\mathcal{N}_i} ||P_j \Delta_{ji}||^2 \leq \frac{\lambda_{min}(Q_i)}{8(|\mathcal{N}_i|+1)}.$$

Moreover, the parameters are $\sigma_i = \sqrt{\alpha_i/\beta_i}$ and must hold

$$0 < \alpha_i < \lambda_{min}(Q_i) - (1+|\mathcal{N}_i|)\delta - \frac{2W_i}{\delta}$$
$$\beta_i = \frac{\|P_i B_i K_i\|^2}{\delta} + \sum_{j\in\mathcal{N}_i}\frac{2\|P_j B_j L_{ij}\|^2}{\delta}$$
$$\delta < \min_i\left\{\frac{\lambda_{min}(Q_i)}{2(1+|\mathcal{N}_i|)}\left(1+\sqrt{1-\frac{8(|\mathcal{N}_i|+1)W_i}{\lambda_{min}^2(Q_i)}}\right)\right\}.$$

Note that the number of constraints are larger and, hence, the design is more complicated.

As far as the inter-execution times, there is now positive lower bound independent of the state $x(t)$ in [257]. Thus, it is unclear what happens when the system approaches the origin. However, the existence of a positive lower bound is guaranteed in [239] at least for the centralized case and linear systems.

7.4.3 Simulation Example

7.4.3.1 System Description

In order to demonstrate the effectiveness of the event-based control strategy, let us consider the system consisting of a collection of N inverted pendulums of mass m and length l coupled by springs with rate k as in Fig. 7.3. This setup will be used throughout this and Chap. 10.

The problem of coupled oscillators has numerous applications in such fields as medicine, physics, or communications [53, 237], and the inverted pendulum is a well-known control engineering problem. The inverted pendulums are physically connected by springs and we desire to design control laws to reach the equilibrium as well as to decouple the system. The state of a pendulum i is broadcast to its neighbors in the chain at discrete times given by the communication strategy.

Each subsystem can be described as follows:

$$\dot{x}_i(t) = \begin{pmatrix} 0 & 1 \\ \frac{g}{l} - \frac{a_i k}{ml^2} & 0 \end{pmatrix} x_i(t) + \begin{pmatrix} 0 \\ \frac{1}{ml^2} \end{pmatrix} u_i + \sum_{j \in \mathcal{N}_i} \begin{pmatrix} 0 & 0 \\ \frac{h_{ij} k}{ml^2} & 0 \end{pmatrix} x_j(t)$$

where $x_i(t) = \begin{pmatrix} x_{i_1}(t) & x_{i_2}(t) \end{pmatrix}^T$ is the state, a_i is the number of springs connected to the ith pendulum, and $h_{ij} = 1, \forall j \in \mathcal{N}_i$ and 0 otherwise.

State-feedback gains and decoupling gains are designed so that the system is perfectly decoupled, and each decoupled subsystem poles are at -1 and -2. This yields the following control law:

$$u_i(t) = \left(-3ml^2 \; a_i k - \frac{ml^2}{4} \left(8 + \frac{4g}{l} \right) \right) x_{b,i}(t) + \sum_{j \in \mathcal{N}_i} \begin{pmatrix} -k & 0 \end{pmatrix} x_{b,j}(t)$$

where $x_{b,i}(t) = \begin{pmatrix} x_{b,i_1}(t) & x_{b,i_2}(t) \end{pmatrix}^T$. In the following, the system parameters are set to $g = 10, m = 1, l = 2,$ and $k = 5$.

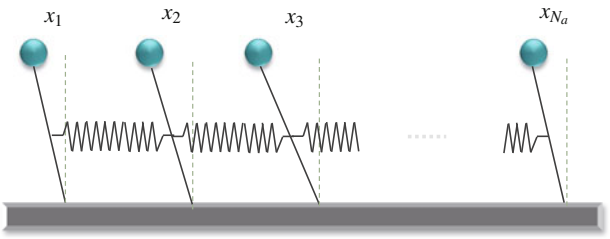

Fig. 7.3 Scheme of the network of the inverted pendulums

7.4.3.2 Performance and Comparison

The output of the system and the sequence of events for $N = 4$ and the same initial conditions than in the previous example when the trigger function is defined as in (7.26) with parameters $\delta_0 = 0.02$, $\delta_1 = 0.5$, and $\beta = 0.8$ are shown in Fig. 7.4.

The convergence of the system to a small region ($\delta_0 = 0.02$) around equilibrium is guaranteed due to the time dependency in the trigger functions. The event generation is shown in Fig. 7.4b. The system converges to zero with few events. Note that the agent that generates the highest number of events is Agent 2 (in red) and this value is 24 over a period of 15 s. Table 7.1 compares the proposed event-triggered approach to periodic control.

The bandwidth of the closed-loop subsystem is 0.8864 rad/s and the sampling period should be between (0.1772, 0.3544) s, according to [74], i.e., (42, 85) transmissions in a 15 s time, whereas the value for the minimum and maximum inter-event times are 0.1690 and 2.260, respectively. Furthermore, this comparison is even unfair with the event-based approach, since once the system is around the equilibrium point, the broadcasting periods take values around 1–2 s.

Observe also that the control signals are piecewise constant (Fig. 7.4c). They are updated if an event is triggered by the agent or its neighbors.

Table 7.2 extends this study for a larger number of agents. Several simulations were performed for different initial conditions for each value of N_a. Minimum and mean values of the inter-event times T_k^i were calculated for the set of the simulations with the same number of agents. We see that the broadcasting period remains almost constant when the number of agents increases. Thus, the amount of communication for the overall network grows linearly with N_a.

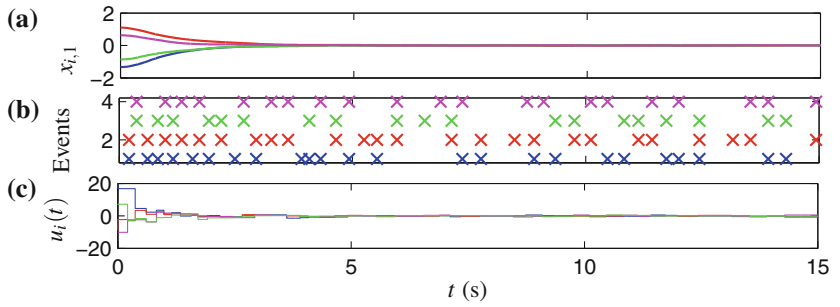

Fig. 7.4 Simulation results with trigger functions (7.26) with $\delta_0 = 0.02$, $\delta_1 = 0.5$, $\beta = 0.8$

Table 7.1 Comparison of time-triggered and event-triggered strategies

	No. updates	$\{T_k^i\}_{min}$ (s)	$\{T_k^i\}_{max}$ (s)
Time-triggered	(42, 85)	0.177	0.3544
Event-triggered	24	0.1690	2.260

Table 7.2 Inter-event times for different N

	N (s)	10	50	100	150	200
Trigger condition (7.26)	$\{T_k^i\}_{min}$	0.053	0.031	0.015	0.019	0.009
	$\{T_k^i\}_{\text{mean}}$	0.565	0.565	0.567	0.572	0.568
Trigger condition (7.24)	$\{T_k^i\}_{min}$	0.008	0.005	0.004	0.002	0.001
	$\{T_k^i\}_{\text{mean}}$	0.183	0.132	0.129	0.121	0.116
Trigger condition of [257]	$\{T_k^i\}_{\text{mean}}$	0.115	0.118	0.115	0.118	0.118

Moreover, these results are compared to other event-trigger functions: (7.24) with $\delta = 0.02$, and (7.25). For this later case, the results are taken from [257]. We see that trigger functions (7.26) can provide around five times larger broadcast periods. For example, for a number of pendulums of $N_a = 100$, trigger functions of the form (7.26) give a mean broadcasting period of 0.567, whereas trigger functions of the form (7.24) provide 0.129 and the result given in [257] is 0.115.

7.5 Extension to Discrete-Time Systems

7.5.1 System Description

The previous analysis considers that the state of the subsystems is monitored continuously. However, in practice, most of the hardware platforms only provide periodical implementations of the measurement and actuation tasks.

Hence, let us consider that each subsystem i is sampled at predefined instances of time given by a sampling period T_s. The discrete-time dynamical equation describing each subsystem is

$$x_i(\ell+1) = A_i x_i(\ell) + B_i u_i(\ell) + \sum_{j \in \mathcal{N}_i} H_{ij} x_j(\ell). \tag{7.34}$$

The control law is given by

$$u_i(\ell) = K_i x_{b,i}(\ell) + \sum_{j \in \mathcal{N}_i} L_{ij} x_{b,j}(\ell), \tag{7.35}$$

where $x_{b,i}(\ell)$ is the last-broadcast state, K_i is the feedback gain, and L_{ij} are the decoupling gains for the discrete-time subsystem i. The error is defined again as the difference between the last-broadcast state and the measured state. Thus,

$$\varepsilon_i(\ell) = x_{b,i}(\ell) - x_i(\ell), \tag{7.36}$$

and (7.34) can be rewritten in terms of the error $\varepsilon_i(\ell)$ as

$$x_i(\ell+1) = A_{K,i}x_i(\ell) + B_iK_i\varepsilon_i(\ell) + \sum_{j\in\mathcal{N}_i} \Delta_{ij}x_j(\ell) + B_iL_{ij}\varepsilon_j(\ell), \tag{7.37}$$

where $A_{K,i} = A_i + B_iK_i$ and $\Delta_{ij} = B_iL_{ij} + H_{ij}$. K_i are designed so that all the eigenvalues of $A_{K,i}$ lie inside the unit circle.

If we define the block matrices A_K, B, K, and Δ as in (7.16)–(7.19), and the stack vectors x and e as in (7.20) and (7.21), respectively, then the overall system dynamics is

$$x(\ell+1) = (A_K + \Delta)x(\ell) + BKe(\ell). \tag{7.38}$$

7.5.2 Discrete-Time Trigger Functions

Trigger functions of the form (7.26) are difficult to implement in digital platforms since they involve a decaying exponential. Therefore, for discrete-time systems, we propose the following functions

$$F_{e,i}(\varepsilon_i(\ell), \ell) = \|\varepsilon_i(\ell)\| - (\delta_0 + \delta_1\beta^{\ell}), \quad 0 < \beta < 1 \tag{7.39}$$

since they can be assimilated to (7.26) for discrete-time instances.

The instances of discrete time at which events are detected are denoted as ℓ_k^i and are defined recursively as follows:

$$\ell_{k+1}^i = \inf\{\ell > \ell_k^i, F_{e,i}(\varepsilon_i(\ell), \ell) \geq 0\}.$$

Example 7.2 Let us consider a trigger function $F_{e,i}(\varepsilon_i(t), t) = \|\varepsilon_i(t)\| - (0.01 + 0.5e^{-0.8t})$ in continuous time t, which bounds the error $\|\varepsilon_i(t)\| \leq (0.01 + 0.5e^{-0.8t})$. This bound is depicted in Fig. 7.5 (blue line). Assume that this system is sampled:

- With a sampling period $T_s = 0.1$.
- With a sampling period $T_s = 0.2$.

Trigger functions of the form (7.39) can be defined with the same values for δ_0 and δ_1 and with $\beta = e^{-0.8T_s}$. This yields values $\beta = 0.9231$ and $\beta = 0.8521$, respectively. The error bounds for both cases are shown in Fig. 7.5. Note that this bound is a piecewise constant function and changes at the sampling time instances.

7.5.3 Stability Analysis

Theorem (7.1) sums up the stability results for the continuous time system. Equivalent results can be derived for the discrete-time system (7.38).

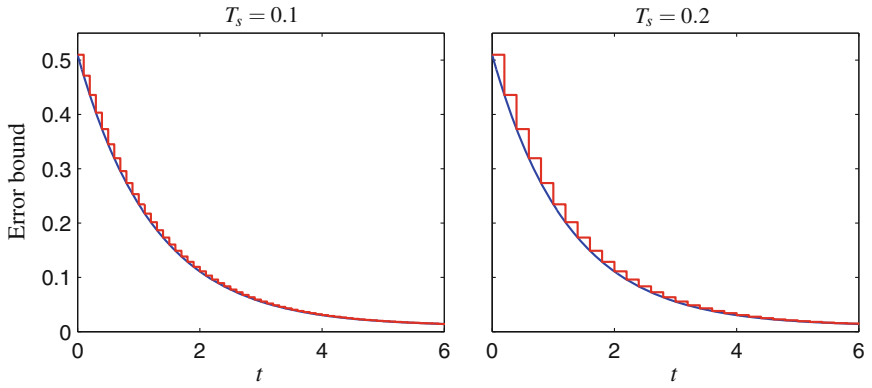

Fig. 7.5 Comparative of time-continuous (*blue*) and discrete-time (*red*) trigger functions, $T_s = 0.1$ (*left*), $T_s = 0.2$ (*right*)

However, a remark should be pointed out first. Whereas in continuous time the state is monitored continuously and this ensures that the error $\varepsilon_i(t)$ is strictly upper bounded by $\delta_0 + \delta_1 e^{-\beta t}$, in discrete-time systems it might occur that for a given ℓ, $\|\varepsilon_i(\ell)\| < \delta_0 + \delta_1 \beta^{\ell}$, but $\|\varepsilon_i(\ell+1)\| > \delta_0 + \delta_1 \beta^{\ell+1}$, so that the error reached the bound in the inter-sampling time.

In order to deal with this phenomenon, we state the following assumption.

Assumption 7.3 Fast sampling is assumed [109] so that events occur in all probability at the sampling times ℓ. Hence, $\|\varepsilon_i(\ell_k^i)\| \approx \delta_0 + \delta_1 \beta^{\ell_k^i}$ for some $\ell = \ell_k^i$.

The next theorem states that the system (7.38), when trigger functions (7.39) are used, converges to a region around the origin, which depends on δ_0.

The proof of the theorem can be found in Appendix A, being two the clues to follow the proof. First, all the eigenvalues of A_K lie inside the unit circle, so that $|\lambda_{max}(A_K)|^{\ell} < 1, \forall \ell \geq 0$ and $|\lambda_{max}(A_K)|^{\ell} \xrightarrow{\ell \to \infty} 0$, being $\lambda_{max}(A_K)$ the maximum of the eigenvalues of A_K. Second, the perturbation analysis for matrix powers, and in particular (7.11), can be applied. Before enouncing the theorem, the following assumption is required:

Assumption 7.4 A_K is diagonalizable so that $A_K = VDV^{-1}$, and the coupling terms are such that $\kappa(V)\|\Delta\| < 1 - |\lambda_{max}(A_K)|$, where $\kappa(V) = \|V\|\|V^{-1}\|$ and $\lambda_{max}(A_K)$ is the eigenvalue of A_K with the closer magnitude to 1. Furthermore, it is assumed that Δ is such that the second-order terms can be approximated to zero $\mathcal{O}(\|\Delta\|^2) \approx 0$.

Note that when $\beta \neq 0$, and additional constraint is imposed to the coupling terms. Specifically, the condition $|\lambda_{max}(A_K)| + \kappa(V)\|\Delta\| < \beta < 1$ ensures the convergence to the equilibria.

Theorem 7.2 *Consider the closed-loop system (7.38) and trigger functions of the form (7.39), where* $|\lambda_{max}(A_K)| + \kappa(V)\|\Delta\| < \beta < 1$. *If Assumptions 7.3 and 7.4 hold, then, for all initial conditions* $x(0) \in \mathbb{R}^n$ *and* $\ell > 0$, *it holds*

$$\begin{aligned}\|x(\ell)\| \leq \kappa(V)\Bigg(&\tfrac{\|BK\|\sqrt{N_a}\delta_0}{1-|\lambda_{max}(A_K)|}\gamma_0 + |\lambda_{max}(A_K)|^{\ell}\Big(\|x(0)\| - \tfrac{\|BK\|\sqrt{N_a}\delta_0}{1-|\lambda_{max}(A_K)|}\gamma_0 \\ &- \tfrac{\|BK\|\sqrt{N_a}\delta_1}{\beta-|\lambda_{max}(A_K)|}\gamma_1 + \tfrac{\kappa(V)\|\Delta\|}{|\lambda_{max}(A_K)|}\ell\left(\|x(0)\| - \tfrac{\|BK\|\sqrt{N_a}\delta_0}{1-|\lambda_{max}(A_K)|} - \tfrac{\|BK\|\sqrt{N_a}\delta_1}{\beta-|\lambda_{max}(A_K)|}\right)\Big) \\ &+ \beta^{\ell}\tfrac{\|BK\|\sqrt{N_a}\delta_1}{\beta-|\lambda_{max}(A_K)|}\gamma_1\Bigg),\end{aligned} \tag{7.40}$$

where

$$\gamma_0 = 1 + \frac{\kappa(V)\|\Delta\|}{1 - |\lambda_{max}(A_K)|} \tag{7.41}$$

$$\gamma_1 = 1 + \frac{\kappa(V)\|\Delta\|}{\beta - |\lambda_{max}(A_K)|}. \tag{7.42}$$

Remark 7.3 If perfect decoupling can be achieved, then $\|\Delta\| = 0$, which yields $\gamma_0, \gamma_1 = 1$. Thus, (7.40) is simplified:

$$\begin{aligned}\|x(\ell)\| \leq \kappa(V)\Bigg(&\tfrac{\|BK\|\sqrt{N_a}\delta_0}{1-|\lambda_{max}(A_K)|} + |\lambda_{max}(A_K)|^{\ell}\Big(\|x(0)\| - \tfrac{\|BK\|\sqrt{N_a}\delta_0}{1-|\lambda_{max}(A_K)|} \\ &- \tfrac{\|BK\|\sqrt{N_a}\delta_1}{\beta-|\lambda_{max}(A_K)|}\Big) + \beta^{\ell}\tfrac{\|BK\|\sqrt{N_a}\delta_1}{\beta-|\lambda_{max}(A_K)|}\Bigg).\end{aligned}$$

7.6 Improvements

The objective of this section is the proposal of some improvements to the design described previously in the chapter. First, a novel implementation is presented to reduce the number of control updates allowing a more efficient usage of the limited resources of embedded microprocessors. In the previous design, the adaption frequency of the control input may be high when the neighborhood is large even if each agent is not transmitting so often. The design is based on two sets of trigger functions. The first set decides when to transmit an update for the broadcast state and the second set checks a predefined control error at broadcasting events, updating only when this error exceeds a given threshold.

The second improvement of the discrete-event-based control (DEBC) has a different goal, which is to reduce as much as possible the communication through the network even if the load of the microprocessor is increased. We present a distributed model-based control design in which each agent has certain knowledge of the dynamics of its neighborhood. Based on this model, the subsystem estimates its state and its neighbors' continuously and computes the control law accordingly. Model uncertainty is assumed and the performance of the Sect. 7.4's and

model-based designs are compared, showing that a model-based controller allows larger inter-event times.

7.6.1 Reducing Actuation in Distributed Control Systems

This section presents a distributed control design where the goal is not only to reduce communication but also the number of control updates in each node. Note that in a single control loop the reduction of communication usually implies the reduction of actuator updates [68, 239], which does not necessary hold in distributed systems.

The control law is computed in (7.13) based on the broadcast states. Thus, $u(t)$ is a piecewise constant function. Accordingly, the control law of agent i is updated when an event is triggered by itself or any of its neighbors. This might lead to very frequent control updates if the number of neighbors was large. However, the change of the control signal $u_i(t)$ might be small due to, e.g., a weak coupling. In this situation, an update of the control signal is generally not needed.

We propose a new control law in which $u_i(t)$ is not updated at each broadcasting event, but when an additional condition is fulfilled. We consider two mechanisms driven by events. The first one is the transmission of information between nodes (*transmission events*), and the second one is the update of the control law (*control update events*). Note that the *transmission events* correspond to the considered events up to now. The description of both sets of trigger functions is given next.

7.6.1.1 Trigger Functions

Transmission Events

The occurrence of a transmission event is defined by trigger functions $F_{x,i}$ which only depend on local information of agent i and take values in $\mathbb{R}$.

The sequence of broadcasting times t_k^i are determined recursively by the event-trigger function as

$$t_{k+1}^i = \inf\{t : t > t_k^i, F_{x,i}(t) > 0\}.$$

We define the error between the current state x_i and the most recently broadcast state $x_{b,i}$ as

$$\varepsilon_{x,i}(t) = x_{b,i}(t) - x_i(t), \tag{7.43}$$

and we consider time-dependent trigger functions defined by

$$F_{x,i}(t, \varepsilon_{x,i}(t)) = \|\varepsilon_{x,i}(t)\| - \delta_{x,0} - \delta_{x,1} e^{-\beta t}, \tag{7.44}$$

with $\delta_{x,0} > 0$, $\delta_{x,1} \geq 0$, and $\alpha > 0$. An event is detected when $F_{x,i}(t, \varepsilon_{x,i}(t)) > 0$, and the error $\varepsilon_{x,i}$ is reset to zero. Note that the error remains bounded by

$$\|\varepsilon_{x,i}(t)\| \leq \delta_{x,0} + \delta_{x,1} e^{-\beta t}. \tag{7.45}$$

This type of trigger functions has been shown to decrease the number of events while maintaining a good performance of the system. The case $\delta_{x,0} = 0$ is excluded. The reason is discussed later. However, the case $\delta_{x,1} = 0$ is admitted leading to static trigger functions.

Control Update Events

Let us denote the time instants at which the control update of the agent i occurs as $\{t_\ell^i\}_{\ell=0}^{\infty}, \forall i = 1, \ldots, N_a$.

The control law is defined for the inter-event time period as

$$u_{b,i}(t) = K_i x_{b,i}(t_\ell^i) + \sum_{j \in N_i} L_{ij} x_{b,j}(t_\ell^i), t \in [t_\ell^i, t_{\ell+1}^i). \tag{7.46}$$

In order to determine the occurrence of an event, we define

$$\varepsilon_{u,i}(t) = u_{b,i}(t) - u_i(t), \tag{7.47}$$

where $u_i(t)$ is given by (7.13). The set of trigger functions is given by

$$F_{u,i}(\varepsilon_{u,i}(t)) = \|\varepsilon_{u,i}(t)\| - \delta_u, \quad \delta_u > 0. \tag{7.48}$$

The sequence of control updates is determined recursively. However, whereas the transmission events can occur at any time t because $x_i(t)$ is a continuous function, $u_i(t)$ in (7.13) is not continuous but piecewise constant and only changes its value at transmission events. This means that the events on the control update are a subsequence of the transmission events.

Denote $\bar{\mathcal{N}_i} = i \cup \mathcal{N}_i$ and $\{t_k^{\bar{\mathcal{N}_i}}\}$ the set $\{t_k^i\} \cup \{t_k^j\}$, $j \in \mathcal{N}_i$. Thus,

$$t_{\ell+1}^i = \inf\{t_k^{\bar{\mathcal{N}_i}} : t_k^{\bar{\mathcal{N}_i}} > t_\ell^i, F_{u,i}(t_k^{\bar{\mathcal{N}_i}}) > 0\}.$$

Hence, it holds that $\{t_\ell^i\} \subset \{t_k^{\bar{\mathcal{N}_i}}\}$.

Example 7.3 An example of the proposed design is given in Fig. 7.6. Assume that Agent 1 sends and receives information to/from its neighborhood through a network. At $t = t_k^2$ it receives a broadcast state $x_{b,2}$ from Agent 2. Agent 1 computes u_1 according to the new value received. For example, if Agent 2 is its unique neighbor, $u_1(t_k^2) = K_1 x_{b,1}(t_k^2) + L_{12} x_{b,2}(t_k^2) = K_1 x_{b,1}(t_{k-1}^1) + L_{12} x_{b,2}(t_k^2)$, where t_{k-1}^1 is assumed to be the last broadcasting event time for Agent 1. After computing u_1, Agent 1 checks whether the difference between this value and the current control signal applied exceeds the threshold δ_u. Since this threshold is not exceeded, it does not update $u_{b,1}$. At $t = t_k^1$, Agent 1 detects an event because εx, 1 reaches the threshold δ_x. $x_1(t_k^1)$ is broadcast through the network and u_1 is computed again. Given that $\|\varepsilon_{u,1}\| < \delta_u$, $u_{b,1}$ is not modified. Finally, a new event occurs at $t = t_{k+1}^1$ resulting in a broadcast and a control update since $\|\varepsilon_{u,1}\| \geq \delta_u$. Note that $u_{b,1}(t) = u_1(t)$.

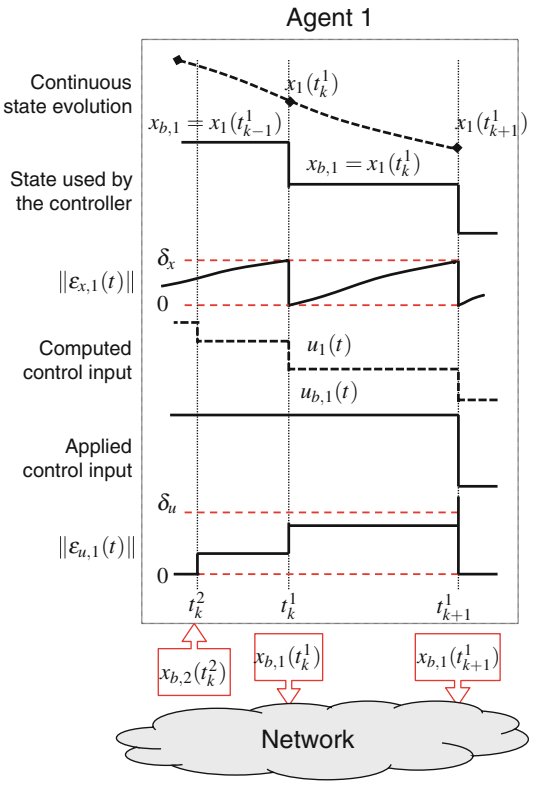

Fig. 7.6 Illustrative example of transmission and control update events between a system compound of two agents

7.6.1.2 Performance Analysis

The dynamics of the subsystems (7.12) with control law (7.46) is

$$\dot{x}_i(t) = A_i x_i(t) + B_i u_{b,i}(t) + \sum_{j \in N_i} H_{ij} x_j(t).$$

It can be rewritten in terms of the errors $\varepsilon_{x,i}(t)$ and $\varepsilon_{u,i}(t)$ handled by the trigger functions (7.44) and (7.48). respectively, as

$$\dot{x}_i(t) = A_{K,i} x_i(t) + \sum_{j \in N_i} \Delta_{ij} x_j(t) + B_i K_i \varepsilon_{x,i}(t) + B_i \sum_{j \in N_i} L_{ij} \varepsilon_{x,j}(t) + B_i \varepsilon_{u,i}(t).$$

Let us define the stack vectors

$$\begin{aligned} \varepsilon_x^T &= \left(\varepsilon_{x,1}^T \dots \varepsilon_{x,N}^T\right) \\ \varepsilon_u^T &= \left(\varepsilon_{u,1}^T \dots \varepsilon_{u,N}^T\right), \end{aligned} \tag{7.49}$$

and consider the usual definitions for $x(t)$ and the matrices A_K, B, K, and Δ given in (7.16)–(7.19).

Accordingly, the overall system dynamics is given by

$$\dot{x}(t) = (A_K + \Delta)x(t) + BK\varepsilon_x(t) + B\varepsilon_u(t). \tag{7.50}$$

As the broadcast states $x_{b,i}$ remain constant between consecutive events, the dynamics of the state error in each interval are given by

$$\dot{\varepsilon}_x(t) = -(A_K + \Delta)x(t) - BK\varepsilon_x(t) - B\varepsilon_u(t). \tag{7.51}$$

The state error of the overall system is bounded by

$$\|\varepsilon_x(t)\| \leq \sqrt{N_a}(\delta_{x,0} + \delta_{x,1}e^{-\beta t})$$

according to (7.45). However, $\varepsilon_u(t)$ is not strictly bounded by δ_u because $u_i(t)$ is not a continuous function but piecewise constant. To find an analytical bound, we assume that that the occurrence of simultaneous transmission events in any neighborhood $\bar{\mathcal{N}_i}$ is not allowed, i.e., two neighboring nodes cannot transmit at the same instance of time. Moreover, in case that two broadcast states were received by one agent simultaneously, it could enqueue the data and do the computation of the control law sequentially. This might induce delays in the case where two nodes attempted to transmit at the same time. However, we assume that this delay is negligible in this section. The effect of delays and packet losses on event-triggered control of distributed control systems will be studied in Chap. 10.

Lemma 7.4 *The control error of the subsystem i is bounded by*

$$\|\varepsilon_{u,i}(t)\| \leq \bar{\delta}_{u,i}(t), \tag{7.52}$$

with

$$\bar{\delta}_{u,i}(t) = \delta_u + (\delta_{x,0} + \delta_{x,1}e^{-\beta t}) \cdot max\{\|K_i\|, \|L_{ij}\| : j \in \mathcal{N}_i\}.$$

Moreover, the control error of the overall system is bounded by

$$\|\varepsilon_u(t)\| \leq \sqrt{N_a}(\delta_u + \|\mu(K)\|_{max}(\delta_{x,0} + \delta_{x,1}e^{-\beta t})) = \bar{\delta}_u(t), \tag{7.53}$$

where

$$\mu(K) = \begin{pmatrix} \|K_1\| & \|L_{12}\| & \cdots & \|L_{1N}\| \\ \|L_{21}\| & \|K_2\| & \cdots & \|L_{2N}\| \\ \vdots & \vdots & \ddots & \vdots \\ \|L_{N1}\| & \|L_{N2}\| & \cdots & \|K_N\| \end{pmatrix}, \tag{7.54}$$

and $\|\cdot\|_{max}$ denotes the entry-wise max norm of a matrix.

Proof The proof can be found in Appendix A.

We next present the main result of the section.

Theorem 7.3 *Consider the interconnected linear system (7.50). If trigger functions (7.44) are used to broadcast the state with* $0 < \beta < |\alpha_{max}(A_K)| - \kappa(V)\|\Delta\|$*, and trigger functions (7.48) for the control update, then, for all initial conditions* $x(0)$ *and* $t \geq 0$*, it follows that*

$$\|x(t)\| \leq \sigma_1 + (\kappa(V)\|x(0)\| - \sigma_1 - \sigma_2)e^{-(|\alpha_{max}(A_K)|-\kappa(V)\|\Delta\|)t} + \sigma_2 e^{-\beta t}, \quad (7.55)$$

where

$$\sigma_1 = \kappa(V)\sqrt{N_a}\frac{(\|BK\| + \|B\|\|\mu(K)\|_{max})\delta_{x,0} + \|B\|\delta_u}{|\alpha_{max}(A_K)| - \kappa(V)\|\Delta\|} \quad (7.56)$$

$$\sigma_2 = \kappa(V)\sqrt{N_a}\frac{(\|BK\| + \|B\|\|\mu(K)\|_{max})\delta_{x,1}}{|\alpha_{max}(A_K)| - \kappa(V)\|\Delta\| - \beta}. \quad (7.57)$$

Furthermore, the system does not exhibit Zeno behavior, being the lower bound for the inter-execution times

$$T_{x,min} = \frac{\delta_{x,0}}{\gamma_1 + \sqrt{N_a}(\gamma_2 + \gamma_3 + \gamma_4)}, \quad (7.58)$$

where

$$\gamma_1 = \kappa(V)\|x(0)\|\|A_K + \Delta\|$$

$$\gamma_2 = (\|BK\| + \|B\|\|\mu(K)\|_{max})\delta_{x,0}\left(1 + \frac{\kappa(V)\|A_K+\Delta\|}{|\alpha_{max}(A_K)|-\kappa(V)\|\Delta\|}\right)$$

$$\gamma_3 = (\|BK\| + \|B\|\|\mu(K)\|_{max})\delta_{x,1}\left(1 + \frac{\kappa(V)\|A_K+\Delta\|}{|\alpha_{max}(A_K)|-\kappa(V)\|\Delta\|-\alpha}\right)$$

$$\gamma_4 = \|B\|\delta_u\left(1 + \frac{\kappa(V)\|A_K+\Delta\|}{|\alpha_{max}(A_K)|-\kappa(V)\|\Delta\|}\right).$$

Proof The proof can be found in Appendix A.

The previous analysis is based on two sets of trigger functions to detect transmission and control updates events. One concern that can be raised is how the values of the parameters of these trigger functions can be selected or if there is any relationship between them.

Let us first assume the case $\delta_{x,1} = 0$ yielding to static trigger functions. It follows that $\|\varepsilon_{x,i}(t)\| \leq \delta_{x,0}$ and $\|\varepsilon_{u,i}(t)\| \leq \delta_u + \delta_{x,0} \cdot \max\{\|K_i\|, \|L_{ij}\| : j \in \mathcal{N}_i\}\ \forall t \geq 0$, according to (7.45) and (7.52), respectively.

Assume that the last control update event occurred at $t = t^*$ and denote the number of transmission events between t^* and the next broadcast as n_e. A lower

bound for n_e can be derived following the ideas of Lemma 7.4:

$$\|\varepsilon_{u,i}(t) - \varepsilon_{u,i}(t^*)\| = \|\varepsilon_{u,i}(t)\| \leq \sum_{k=1}^{n_e} \delta_{x,0} \cdot \max\{\|K_i\|, \|L_{ij}\| : j \in \mathcal{N}_i\}$$
$$= n_e \delta_{x,0} \max\{\|K_i\|, \|L_{ij}\| : j \in \mathcal{N}_i\}$$

and the next control update event will not be triggered before

$$\|\varepsilon_{u,i}\| = \delta_u \leq \delta_u + \delta_{x,0} \max\{\|K_i\|, \|L_{ij}\| : j \in \mathcal{N}_i\}.$$

Thus,

$$n_e^i \geq \frac{\delta_u}{\delta_{x,0} \max\{\|K_i\|, \|L_{ij}\| : j \in \mathcal{N}_i\}}. \tag{7.59}$$

Equation (7.59) shows the trade-off between δ_u and $\delta_{x,0}$ and gives insights on how one of these parameters should be chosen according to the other one.

Moreover, (7.59) can be translated into a relationship between the inter-execution times of the control law (7.46), denoted $T_{u,min}^i$, and the minimum broadcasting period (7.58). It holds that

$$T_{u,min}^i \geq n_e^i T_{x,min} \geq \frac{\delta_u}{(\gamma_1 + \sqrt{N_a}(\gamma_2 + \gamma_4)) \max\{\|K_i\|, \|L_{ij}\| : j \in \mathcal{N}_i\}}.$$

Note that $\gamma_3 = 0$ because we are analyzing the case $\delta_{x,1} = 0$. Let $T_{u,min}$ be $T_{u,min} = \min\{T_{u,min}^i\}$. It yields

$$T_{u,min} \geq \frac{\delta_u}{(\gamma_1 + \sqrt{N_a}(\gamma_2 + \gamma_4)) \|\mu(K)\|_{max}}.$$

Hence, $\delta_{x,0}$ and δ_u can be chosen to meet some constraints on $T_{x,min}$ and $T_{u,min}$.

In the design of Sect. 7.6.1.1 the case $\delta_{x,0} = 0$ was excluded and the reason is given next. Assume that $\delta_{x,0} = 0$. Thus, following the steps of the previous case, $\|\varepsilon_{u,i}(t)\| \leq n_e \delta_{x,1} e^{-\beta t^*} \max\{\|K_i\|, \|L_{ij}\| : j \in \mathcal{N}_i\}$, where n_e is the number of broadcasting events and t^* the time of the last control update event. Moreover, the next event is not triggered before $\|\varepsilon_{u,i}\|$ reaches the threshold δ_u. In this case, it holds that

$$n_e \geq \frac{\delta_u}{\delta_{x,1} e^{-\beta t^*} \max\{\|K_i\|, \|L_{ij}\| : j \in \mathcal{N}_i\}}. \tag{7.60}$$

Note that the lower bound for n_e in (7.60) goes to infinity when $t^* \to \infty$, which means that when the time values are large, many transmission events are required to trigger a new control update and may lead to small inter-event times. One possible solution is to accommodate the threshold δ_u to the decreasing bound on the state $\delta_{x,1} e^{-\beta t}$.

7.6.1.3 Simulation Example

Let us consider the system presented in Sect. 7.4.3 but with a different topology. Specifically, the mesh of inverted pendulums is depicted in Fig. 7.7. The dynamics of the subsystem change in this scheme, and three types of agents can be distinguished: the ones in the corners with two neighbors, the ones in the borders (excluding the corners) with three neighbors, and the inner pendulums with four nodes to communicate with. Moreover, movement is assumed to be in the XY plane. Hence, the dimension of the state is $n = 4$ and there are two control inputs ($m = 2$), which are the forces acting in the X and Y directions, respectively.

Figure 7.8 shows the output of the system in a 3D space for a mesh of 6×6 pendulums. The coordinates in the XY plane over time are plotted. Trigger functions with $\delta_{x,0} = 0.02$, $\delta_{x,1} = 0.5$, $\beta = 0.6$, and $\delta_u = 0.1$ are considered.

Let us focus on one particular subsystem, for example the agent (2,2) (second row, second column). The number of broadcasting events in all the neighborhood of this particular agent, which has four neighbors, is 170, while the number of control updates in the agent (2,2) is 90, so that 47 % of the transmissions do not end into a control update because the threshold δ_u is not reached.

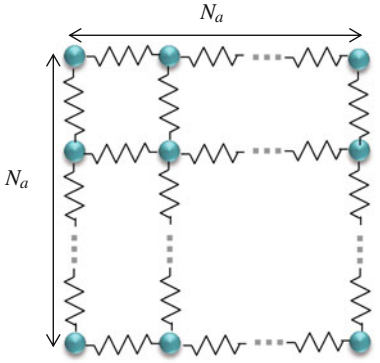

Fig. 7.7 Scheme of the coupled pendulums mesh

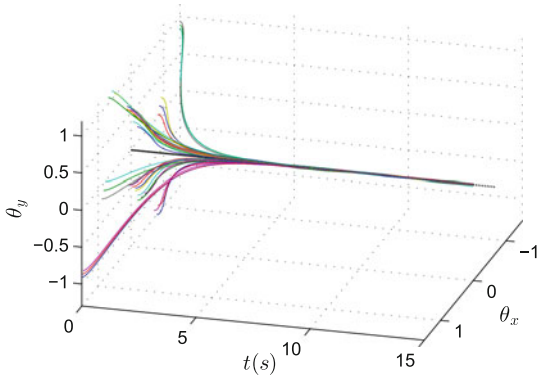

Fig. 7.8 $x_{i_1}(\theta_x)$ and $x_{i_3}(\theta_y)$ for a 6×6 mesh of inverted pendulums

If this experiment is repeated for the case in which trigger functions (7.48) are not considered, the number of broadcasting events in the neighborhood of (2,2) is 140, which is equal to the number of control updates. Thus, the proposed design with trigger functions (7.48) as expected might cause an increase of network transmissions, in this case 21 % while saving almost half of the changes on the control signal. Moreover, if we compute the average broadcasting period for the entire network as $\bar{T}_x = \frac{N_a^2 t_{sim}}{\text{No. events}}$ it yields 0.5202 s for the first case and 0.5954 s for the case without using the event-triggered control update. Hence, for the overall network the difference is not relevant. These results are extended for different values of N_a in Table 7.3. Note that the variations of the average period with the number of agents are not significant.

The influence of the parameter δ_u for given parameters $\delta_{x,0} = 0.02$, $\delta_{x,1} = 0.5$, and $\beta = 0.6$ can be analyzed and the results are illustrated in Table 7.4. For a mesh of 6×6 subsystems, the following values are computed for each value of δ_u and simulation time $t = 15$ s:

- Average number of transmissions through the network defined as $\bar{n}_x = \frac{\sum_{i=1}^{N_a^2} |\{t_k^i\}|}{N^2} |\overline{\mathcal{N}_i}|$, where $|\{t_k^i\}|$ is the cardinality of the set $\{t_k^i\}$ and $|\overline{\mathcal{N}_i}|$ is the average for the number of neighboring agents.
- Average number of control updates defined as $\bar{n}_u = \frac{\sum_{i=1}^{N_a^2} |\{t_\ell^i\}|}{N_a^2}$.

Note that the best choice of the values of δ_u, $\delta_{x,0}$ and $\delta_{x,1}$ depends on the communication and actuation costs of the implementation, and the lower bounds on the inter-event times that should be guaranteed in the system. We can say that a value $\delta_u \in [0.05, 0.1]$ would be a good option because the decrease of the control events is notable while the increase in communication events is assumable. If $\delta_u = 0.02$ all broadcasting events lead into a control update ($\bar{n}_u$ is actually larger than $\bar{n}_x$, but this is due to the error induced by the statistical treatment of the data).

Table 7.3 Average broadcasting period variations with N_a

$N_a \times N_a$	16	36	64	81	100
$\bar{T}_x$	0.5422	0.5202	0.4813	0.4676	0.4765

Table 7.4 Average transmission and control update events with c_u

δ_u	0.02	0.05	0.1	0.2
$\bar{n}_x$	86.20	83.98	95.46	181.48
$\bar{n}_u$	93.11	75.00	67.28	57.58

7.6.2 Model-Based Design

Model-based event-triggered control has been shown to reduce the amount of communication in a control loop [154]. Ideally, if the plant is stable, there are no model uncertainties or external disturbances, the control input $u(t)$ can be determined in a feedforward manner, and no communication over the feedback link is necessary [139].

The distributed approach presented in this section shows that if the model uncertainty fulfills a certain condition, the model-based approach gives larger minimum inter-event times than the zero-order hold approach of Sect. 7.4. We assume that each agent has knowledge of the dynamics of its neighborhood.

In particular, let us define the model-based control law for each agent as

$$u_i(t) = K_i x_{m,i}(t) + \sum_{j \in \mathcal{N}_i} L_{ij} x_{m,j}(t), \tag{7.61}$$

where $x_{m,i}$ now represents the state estimation of x_i given by the model $(A_{m,i}, B_{m,i})$ of each agent, and $A_{mK,i} = A_{m,i} + B_{m,i}K_i$. Let us define $A_{mK} = \text{diag}(A_{mK,1}, \ldots, A_{mK,N_a})$.

The error $\varepsilon_i(t)$ is redefined as

$$\varepsilon_i(t) = x_{m,i}(t) - x_i(t), \tag{7.62}$$

and is reset at events' occurrence. In particular, $x_{m,i}(t)$ is computed in the inter-event times as

$$x_{m,i}(t) = e^{A_{mK,i}(t-t_k^i)} x_i(t_k^i), \quad \forall t \in [t_k^i, t_{k+1}^i). \tag{7.63}$$

Note that (7.63) does not include the coupling effect since the decoupling gains L_{ij} are designed to compensate the model of the interconnections H_{ij}. Thus, if $\Delta_{ij} \neq \mathbf{0}$ it is because these interconnections are partially unknown or perfect decoupling may not be possible due to, e.g., the matrix B_i not having full rank.

Therefore, each agent i has a model of its dynamics and of its neighborhood $\mathcal{N}_i$. Based on this model, it estimates its state denoted as $x_{m,i}(t)$ to compute $u_i(t)$ in (7.61). This idea is illustrated in Fig. 7.9. Note that this is an extension of a conventional model-based controller. In the distributed approach, the controller C has $\mathcal{N}_i + 1$ inputs and one output. A block that represents the model of a subsystem is reset when a new broadcast state is received.

When the state estimation $x_{m,i}(t)$ differs a given quantity from $x_i(t)$, which depends on the trigger function, a new event is generated and the estimation is reset to the new measured state. For instance, $x_{m,i}$ might deviate from x_i due to model uncertainties on $A_{K,i}$, disturbances, and the effect of the non-perfect decoupling. Furthermore, the agent i broadcasts the new measurement to its neighbors, which also update their estimations according to the new value received from agent i.

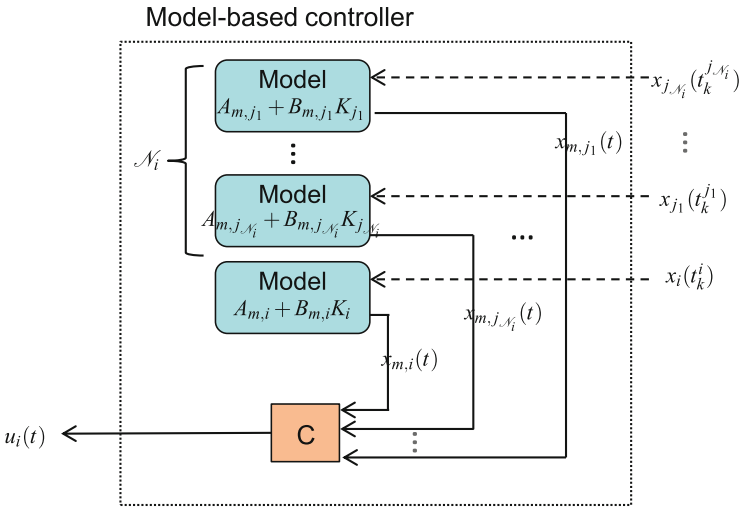

Fig. 7.9 Model-based control scheme for the node i

7.6.2.1 Main Result

If we consider the trigger function defined in (7.26) and for the new error defined in (7.62), the state will be also bounded by (7.28). However, the lower bound for the inter-event time will have a different expression.

Definition 7.2 Let us define

$$\begin{aligned} \delta A &:= A_m - A \\ \delta B &:= B_m - B \\ \delta A_K &:= A_{mK} - A_K = \delta A + \delta B K, \end{aligned} \tag{7.64}$$

i.e., the model uncertainty of the overall system without interconnections.

Assumption 7.5 We assume that the values of δ_0 and δ_1 and the initial conditions $x(0)$ satisfy the following constraint:

$$\frac{\sqrt{N_a}(\delta_0 + \delta_1)}{\|x(0)\| + \frac{\|BK\|\sqrt{N_a}\delta_0}{\alpha_\Delta} + \frac{\|BK\|\sqrt{N_a}\delta_1}{\alpha_\Delta - \beta}} < \kappa(V)\frac{\|A_K + \Delta\| - \|\delta A_K\| - \|\Delta\|}{\|A_{mK}\|}, \tag{7.65}$$

where $\alpha_\Delta = |\alpha_{max}(A_K)| - \kappa(V)\|\Delta\|$.

Remark 7.4 Equation (7.65) is feasible only if the right-hand side is strictly positive, since $\delta_0 + \delta_1 > 0$. This gives a maximum value of the model uncertainty for a given bound on the norm of the coupling terms matrix or vice versa.

Theorem 7.4 *If Assumption 7.5 holds, the lower bound of the broadcasting period for the system (7.22), under the control law (7.61), and with triggering functions (7.26),* $0 < \beta < |\alpha_{max}(A_K)| - \kappa(V)\|\Delta\|$*, is greater than (7.29).*

Proof The proof can be found in Appendix A.

7.6.2.2 Simulation Example

Next, the performance of the model-based approach is demonstrated and compared to the results of Sect. 7.4.3. Let us consider trigger functions $F_{e,i}(t, \varepsilon_i(t)) = 0.02 + 0.5e^{-0.8t}$. Figure 7.10 compares the output of Agent 1 of a chain of four inverted pendulums. Observe that, for this case, the model-based approach reduces the number of events in more than a third (from 23 (in red) to 9 (in blue)). Note that the control law is not a constant piecewise function.

Table 7.5 compares the results of the first row of Table 7.2 with the model-based design. Note that when the controller uses a model, the average and the minimum values of the inter-event times are enlarged, as predicted by Theorem 7.4.

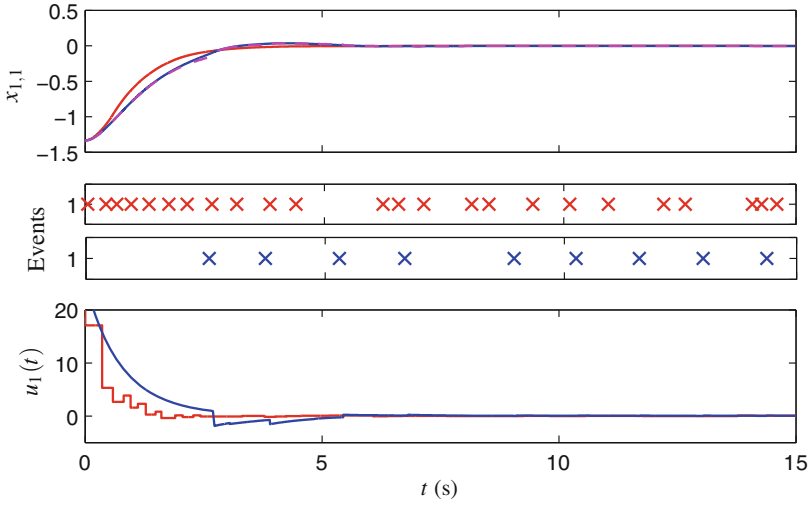

Fig. 7.10 Simulation result with trigger functions (7.26) for the design of Sect. 7.4 (*red*) and the distributed model-based control (*blue*). The *dashed line* (*magenta*) represents the piecewise function $x_{m1,1}$

Table 7.5 Inter-event times for different N_a

	N_a (s)	10	50	100	150	200
Trigger condition (7.26), Sect. 7.4	$\{T_k^i\}_{min}$	0.053	0.031	0.015	0.019	0.009
	$\{T_k^i\}_{\text{mean}}$	0.565	0.565	0.567	0.572	0.568
Trigger condition (7.26), MB control	$\{T_k^i\}_{min}$	0.6816	0.3025	0.219	0.0963	0.132
	$\{T_k^i\}_{\text{mean}}$	1.430	1.500	1.477	1.668	1.581

7.7 Conclusions

A distributed event-based control strategy for interconnected subsystems has been presented. The events are generated by the agents based on local information only, broadcasting their state over the network. The proposed trigger functions preserve the desired convergence properties and guarantee the existence of a strictly positive lower bound for the broadcast period, excluding the Zeno behavior.

Because most of the hardware platforms only provide periodical implementations of the measurement and actuation tasks, the analysis has been extended to discrete-time systems.

Additionally, the way in which the actuation rate can be reduced in an interconnected system if triggering functions are also used in the update of the control law has been illustrated. The existing trade-off between communication and actuation has been shown analytically and through simulations.

Finally, a model-based approach has been proposed showing that the minimum inter-event times can be enlarged if the model uncertainty satisfies certain conditions.